Heat generation associated with pressure-induced infiltration in a nanoporous silica gel

Aijie Han, Venkata K. Punyamurtula, and Yu Qiao[a)]
Department of Structural Engineering, University of California–San Diego, La Jolla, California 92093-0085

(Received 1 December 2007; accepted 18 March 2008)

As a liquid moves in the nanopores of a silica gel, because of the hysteresis of sorption behavior, significant energy dissipation can take place. Through a calometric measurement, the characteristics of associated heat generation are investigated. The temperature variation increases with the mass of silica gel, which consists of a reversible part and an irreversible part. The residual temperature change is about 30% to 60% of the maximum temperature increase and can be accumulated as multiple loading cycles are applied.

I. INTRODUCTION

The recent development of nanoporous materials has provided a novel energy-absorption mechanism for high-performance protection and damping systems.[1–4] When nanoporous particles are immersed in a liquid phase, if the nanopore surfaces are wettable, the liquid would enter the nanopores spontaneously, so that the system free energy decreases.[5] The free-energy change can be estimated as $\Delta U = \Delta\gamma \cdot A$, where $\Delta\gamma$ is the solid–liquid interfacial tension and A is the nanopore surface area. This phenomenon has been widely applied for separation and purification, chemical sensing, catalysis, etc.[6,7] If the nanopore surfaces are nonwettable, an external pressure needs to be applied to trigger liquid infiltration, which would result in an increase in system free energy. The free-energy change is much larger than that of many conventional energy-absorption materials, since the total nanopore surface area, A, can be ultrahigh.[8–11]

For a nanoporous material of nonwettable surface, if the confined liquid defiltrates immediately after the external pressure is reduced, i.e., if the sorption curve is nonhysteretic, the mechanical work that is converted to solid–liquid interfacial tension can be fully released. Thus, the net dissipated energy in a loading–unloading cycle is close to zero. Such a system cannot be used in a protective device, while it may be useful for active control.[12–14] For a number of nanoporous materials, it has been observed that the confined liquid tends to be "locked" inside the nanopores. As the external loading is lowered, defiltration cannot take place instantaneously, unless the external pressure is much lower than the infiltration pressure. That is, the sorption curve is highly hysteretic. Consequently, there is a net energy "loss" in each infiltration–defiltration loop.

One question that still remains unanswered is: what is the mechanism of energy dissipation associated with the nanofluidic motion. Usually, as mechanical work is dissipated, the system entropy would increase, causing a heat generation. However, previous experimental observations[15,16] and computer simulations[17] suggested that in a nanopore or a nanotube, the effective viscosity of confined liquid can be much smaller than the bulk value. As mechanical work is converted to interfacial tension, the interactions among solid and liquid atoms and molecules are dominated by van der Waals and Coulomb force fields, both of which are nondissipative. To understand the energy exchange at the nanometer scale, the characteristics of temperature variation must be adequately understood.

II. EXPERIMENTAL

To monitor the temperature change during pressure-induced infiltration, a high-pressure calometric measurement system was developed, as depicted in Fig. 1(a). The testing cylinder consisted of a stainless steel outer shell and a Teflon inner shell. A steel piston, which was sealed by a reinforced gasket and insulated by a Teflon layer, could be compressed into the cylinder by an external pressure, P. The cylinder contained nanoporous silica gel particles suspended in 4 g of saturated aqueous solution of sodium chloride. The mass of nanoporous silica gel was in the range of 0.1 to 1.0 g. It was obtained from Sigma-Aldrich (St. Louis, MO), with the average nanopore size of 8 nm and the specific nanopore volume of 0.5 cm^3/g. The as-received material had a particle size

[a)]Address all correspondence to this author.
e-mail: yqiao@ucsd.edu
DOI: 10.1557/JMR.2008.0236

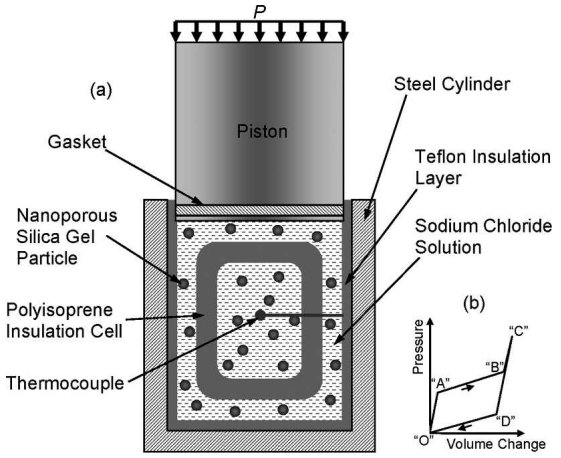

FIG. 1. Schematic diagrams of (a) the experimental setup and (b) the sorption curve.

of about 50 μm. It was first degassed in vacuum at 100 °C for 12 h and then refluxed in 2.5% dry toluene solution of chlorotrimethylsilane (CTMS) at 90 °C for 48 h. Since CTMS molecules were much smaller than the nanopore size, they could react with the hydroxyl sites at nanopore surfaces, forming a monolayer of silane groups.[18,19] Finally, the material was washed by toluene and dried in a vacuum furnace at 100 °C for 12 h. A part of the silica gel suspension was sealed in a polyisoprene (PI) cell, which was immersed in the rest of the suspension in the testing cylinder. The PI cell as well as the liquid phase outside it acted as additional insulation media. Inside the PI cell, the temperature was recorded by a type E thermocouple. The heat capacities of the silica gel suspensions were 4.0, 3.9, 3.8, 3.7, and 3.5 J/g·K, as the silica gel masses were 0.1, 0.25, 0.5, 0.75, and 1.0 g, respectively.

In a type 5580 Instron (Norwood, MA) machine, the piston was driven downward at a constant rate. The loading rate ranged from 0.5 to 30 mm/min. The cross-sectional area of the piston, A_0, was 286 mm^2. The quasi-static pressure in the liquid phase, P, was calculated as the piston force divided by A_0. The volume change of the silica gel suspension was calculated as the piston displacement multiplied by A_0. Unloading was performed at the same rate after P exceeded 50 MPa. Figure 2 shows typical pressure–time and temperature–time curves. For each set of loading rate and silica gel mass, three to four samples were tested, and the results of temperature variations are shown in Figs. 3 and 4. For each sample that contained 0.75 g of silica gel, at the loading rate of 2 mm/min, the infiltration–defiltration loops were repeated 10 times.

III. RESULTS AND DISCUSSION

Since the silane group coated nanopore surface is non-wettable, the nanopores would remain empty as the

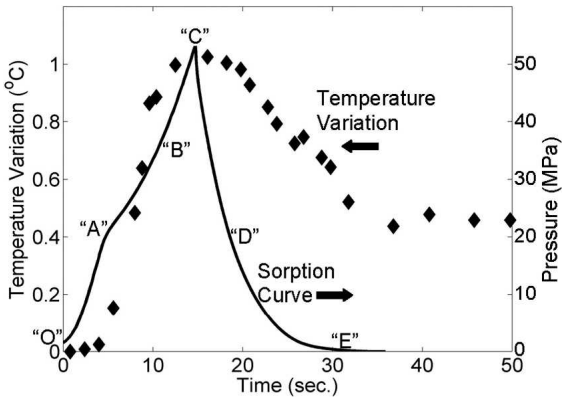

FIG. 2. The temperature and the pressure profiles of a system containing 750 mg of silica gel. The loading rate is 8 mm/min.

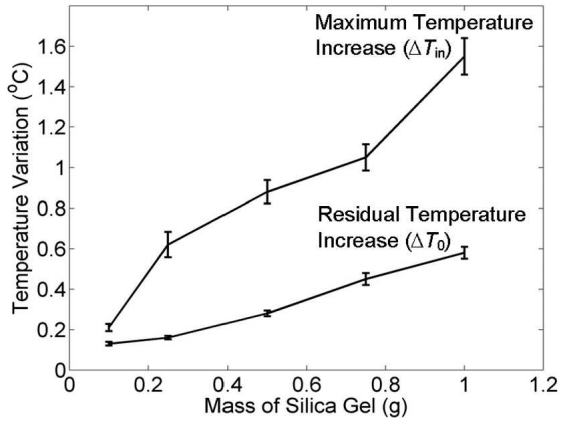

FIG. 3. The temperature variation as a function of the mass of silica gel. The loading rate is 2 mm/min.

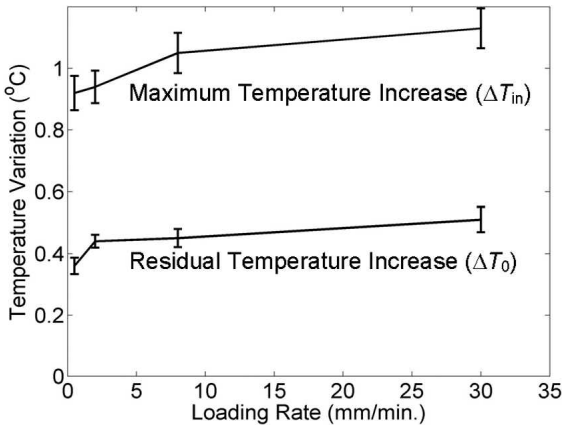

FIG. 4. The temperature variation as a function of the loading rate. The mass of silica gel is 750 mg.

nanoporous silica gel is immersed in water. With the addition of sodium chloride, the effective degree of hydrophobicity is further increased,[20] and the difficulty in defiltration is much reduced.[21] As depicted in Fig. 1(b), if the external pressure applied by the piston is relatively low, the silica gel suspension is rigid, with the compressibility dominated by the free liquid phase. When P

reaches the critical value to overcome the capillary effect, infiltration is induced and an infiltration plateau is formed in sorption curve ("AB"). After the nanopores are filled, the slope of section "BC" is similar to that of "OA." During unloading, defiltration happens at a pressure level much lower than that at "A," leading to a linear return section, "CD." From "D" to "O," as the confined liquid comes out, there is a defiltration plateau. After the first loading–unloading cycle, the sorption curves are nearly identical in all the following cycles. More detailed discussion on sorption–desorption behaviors of the nanoporous silica gel have been given elsewhere.[22] Because of the large deformability of the insulation layers and PI cells, in the current study the onset and ending sections of infiltration and defiltration plateaus are relatively unclear, compared with previous results of steel testing cells.[22] Nevertheless, effective transition points can be defined at the locations where the slopes of sorption curve equal the average values of the slopes in Sections "OA" and "AB."

In such a hysteretic sorption–desorption process, the absorbed mechanical work equals the area enclosed by the loading–unloading cycle, which is nearly 11 J per gram of silica gel.[22] If it is dissipated as heat, for the system containing 0.75 g of silica gel, it would result in a temperature increase $\Delta T_0 = 0.48$ °C. Figure 2 shows that, during infiltration, in section "AB," the temperature indeed largely increases. However, the temperature change, ΔT_{in}, is nearly 1 °C, almost two times higher than the predicted value. Before the infiltration starts, in Section "OA," the temperature variation is negligible, confirming that the elastic compression of free liquid phase and empty nanoporus silica gel particles is isothermal. After the infiltration is complete, but before the defiltration begins, from "B" to "D," the temperature variation is also small; that is, loading and unloading on filled nanoporous silica gel suspension would not cause heat generation or loss. As the confined liquid comes out of the nanopores, during the defiltration plateau ("DE"), temperature decreases, after which, at rest, the system temperature does not vary. The temperature decrease in "DE," ΔT_{de}, is smaller than the temperature increase in "AB." Consequently, after the loading–unloading cycle, there is a net residual temperature variation of 0.45 °C, close to the value of ΔT_0 estimated from the dissipated mechanical work.

Clearly, there are two parts of the temperature increase in infiltration: one is reversible, and the other is irreversible. The reversible part is recovered during defiltration, and the irreversible part leads to the residual temperature variation; that is, $\Delta T_{in} \approx \Delta T_{de} + \Delta T_0$. Both ΔT_{in} and ΔT_0 are linear to the mass of silica gel, m. As shown in Fig. 3, when m is only 0.1 g, ΔT_0 is about 0.1 °C and ΔT_{in} is around 0.2 °C. When $m = 0.5$ g, they are 0.3 and 0.9 °C, respectively. When $m = 1$ g, they become 0.6 and 1.5 °C, respectively. According to the energy dissipation calculated from the sorption curves, the residual temperature changes should respectively be 0.07, 0.17, 0.33, 0.48, and 0.64 °C, for systems of silica masses of 0.1, 0.25, 0.5, 0.75, and 1.0 g, which are close to the measured ΔT_0. The slight nonlinearity may be caused by the change in specific heat. In all the systems, the residual temperature changes are 30% to 60% of the maximum temperature increases, suggesting that the magnitudes of the two parts are comparable. The correlation between temperature variation and silica mass indicates that the exothermic and endothermic processes are related to liquid infiltration and defiltration in nanopores.

Note that, although the temperature change in a single loading cycle is relatively small, for damping systems that work under cyclic loadings the heat generation must be taken into consideration. Because the confined liquid can defiltrate after the external pressure is reduced, after a full cycle of loading and unloading, the system would return to its initial configuration. If similar cycles are applied, it can work continuously. During each loading cycle, the characteristics of temperature change are identical. As a result, the temperature keeps increasing by ΔT_0 in each loop. After only a few cycles, the overall temperature changes by 3 to 4 °C. That is, the nanoporous silica gel suspension acts as a heat source, converting mechanical work to thermal energy.

Figure 4 shows that both ΔT_{in} and ΔT_0 are insensitive to the loading rate. As the loading rate increases from 0.5 to 30 mm/min, the variations of maximum and residual temperature variations are less than 10%. In the range of 2 to 30 mm/min, few statistically meaningful changes can be observed, which suggests that the liquid motion in nanopores is relatively nonviscous, as observed in computer simulations and experiments on nanotubes and nanopores.[23–26] The weak loading rate dependence of temperature change may not be intrinsic. As the loading rate is smaller, it takes longer to complete an infiltration–defiltration loop, and thus the loss of generated heat increases. Moreover, at a higher loading rate, the compression of silica gel suspension can be less regular, causing shear flow among different sections of the liquid phase. Because of the friction of silica gel particles, a certain amount of energy can be dissipated, somewhat similar with the loading rate effect in a shear thickening liquid.[27,28]

The reversible part of temperature variation may be related to the resistance to the motion of liquid molecules. As a liquid molecule moves along a large solid surface, its distance to the solid atoms tends to vary.[29] At a tetrahedral site, the liquid–solid distance is smaller, since the resultant forces from the solid phase reaches the minimum value. In between tetrahedral sites, the liquid molecule moves toward the interior, so that the energy barrier is reduced. In a nanopore, however, the motion of

liquid molecules normal to the solid surface is considerably constrained.[30] Thus, the effect of the energy barrier becomes more pronounced. To overcome the energy barrier, the system free energy must increase by the external pressure. As the energy barrier is bypassed, the excess kinetic energy of the liquid molecule may be absorbed by the adjacent solid atoms to keep the effective infiltration rate constant. During this process, heat is generated and the system temperature increases. During defiltration, the confined liquid molecules bypass the energy barrier with the aid of thermal vibration, and thus they absorb heat from the environment, causing a temperature decrease. Since the energy barrier is independent of the direction of liquid molecule motion, the associated temperature increase and decrease should be the same.

The irreversible part of temperature variation may be associated with the nonlinear relationship between the mobility of confined liquid molecules and the applied pressure, which makes the infiltration and defiltration process hysteretic. It may also be attributed to the imperfect nanopore structure. For instance, if the nanopore diameter varies in a certain range, across a "bottleneck" site the liquid motion can be different with or without an external pressure, resulting in additional hysteresis. Furthermore, the silane groups that cover the nanopore surface may not be uniform. Their density may be higher close to the open end of a nanopore and lower in the interior. Thus, since infiltration starts from the outside and defiltration starts from inside, the loading and unloading paths tend to be different. The role of entrapped gas molecules in nanopores can also be fundamentally different from that in larger pores,[31,32] which may either block or promote infiltration and defiltration, depending on the nanoporous structure, the host and guest species, as well as the working pressure.

IV. CONCLUDING REMARKS

It is clear that the previous discussion is qualitative. A number of details, such as the force fields governing liquid motion, the liquid structures across a tetrahedral site, the heat transfer in nanopore walls, etc., are still under investigation. The experimental data reported in this article provide a basis for further theoretical and simulation analyses. It is shown that temperature varies as liquid moves in nanopores. The temperature variation has a reversible part and an irreversible part. Both parts are nearly proportional to the mass of silica gel. The irreversible part can be accumulated as the loading–unloading cycles continue, while the reversible part cannot.

ACKNOWLEDGMENTS

This work was supported by the Army Research Office under Grant No. W911NF-05-1-0288. The authors are also grateful to Professor Vistasp M. Karbhair and Dr. Guijun Xian for the help with the measurement of specific heat.

REFERENCES

1. B. Lefevre, A. Saugey, J.L. Barrat, L. Bocquet, E. Charlaix, P.F. Gobin, and G. Vigier: Intrusion and extrusion of water in highly hydrophobic mesoporous materials—Effects of the pore structure. *J. Chem. Phys.* **120,** 4927 (2004).
2. F.B. Surani, X. Kong, and Y. Qiao: Two staged sorption isotherm of a nanoporous energy absorption system. *Appl. Phys. Lett.* **87,** 251906 (2005).
3. F.B. Surani, X. Kong, D.B. Panchal, and Y. Qiao: Energy absorption of a nanoporous system subjected to dynamic loadings. *Appl. Phys. Lett.* **87,** 163111 (2005).
4. L. Coiffard and V. Eroshenko: Temperature effect on water intrusion/extrusion in grafted silica gels. *J. Colloid Interface Sci.* **300,** 304 (2006).
5. D. Dubbeldam and R.Q. Snurr: Recent development in the molecular modeling of diffusion in nanoporous materials. *Mol. Simul.* **33,** 305 (2007).
6. Y. Lei, W.P. Cai, and G. Wilde: Highly ordered nanostructures with tunable size, shape and properties—A new way to surface nanopatterning using ultra-thin alumina masks. *Prog. Mater. Sci.* **52,** 465 (2007).
7. A. Zukal: Recent trends in the synthesis of nanoporous materials. *Chem. Listy* **101,** 208 (2007).
8. A. Han and Y. Qiao: Pressure induced infiltration of aqueous solutions of multiple promoters in a nanoporous silica. *J. Am. Chem. Soc.* **128,** 10348 (2006).
9. X. Chen, F.B. Surani, X. Kong, V.K. Punyamurtula, and Y. Qiao: Energy absorption performance of steel tubes enhanced by a nanoporous material functionalized liquid. *Appl. Phys. Lett.* **89,** 241918 (2006).
10. F.B. Surani, A. Han, and Y. Qiao: An experimental investigation on pressurized liquid in confining nanoenvironment. *Appl. Phys. Lett.* **89,** 093108 (2006).
11. V.K. Punyamurtula, A. Han, and Y. Qiao: An experimental investigation on a nanoporous carbon functionalized liquid damper. *Philos. Mag. Lett.* **86,** 829 (2006).
12. Y. Qiao, V.K. Punyamurtula, A. Han, X. Kong, and F.B. Surani: Temperature dependence of working pressure of a nanoporous liquid spring. *Appl. Phys. Lett.* **89,** 251905 (2006).
13. A. Han and Y. Qiao: Thermal effects on infiltration of a solubility sensitive volume memory liquid. *Philos. Mag. Lett.* **87,** 25 (2007).
14. A. Han and Y. Qiao: A volume memory liquid. *Appl. Phys. Lett.* **91,** 173123 (2007).
15. B.J. Hinds, N. Chopra, T. Rantell, R. Andrews, V. Ravalas, and L.G. Bachas: Aligned multiwalled carbon nanotube membranes. *Science* **303,** 62 (2004).
16. A.A. Gusev and O. Guseva: Rapid mass transport in mixed matrix nanotube/polymer membranes. *Adv. Mater.* **19,** 2672 (2007).
17. Y.H. Xie, Y. Kong, H.J. Gao, and A.K. Soh: Molecular dynamics simulation of polarizable carbon nanotubes. *Comput. Mater. Sci.* **40,** 460 (2007).
18. A. Han and Y. Qiao: Effects of nanopore size on properties of modified inner surfaces. *Langmuir* **23,** 11396 (2007).
19. A. Han and Y. Qiao: Controlling infiltration pressure of a nanoporous silica gel via surface treatment. *Chem. Lett. (Jpn.)* **36,** 882 (2007).
20. X. Kong, F.B. Surani, and Y. Qiao: Energy absorption of nanoporous silica particles in aqueous solutions of sodium chloride. *Phys. Scr.* **74,** 531 (2006).

21. F.B. Surani and Y. Qiao: Pressure induced infiltration of an epsomite-silica system. *Philos. Mag. Lett.* **86,** 253 (2006).
22. X. Kong and Y. Qiao: Improvement of recoverability of a nanoporous energy absorption system by using chemical admixture. *Appl. Phys. Lett.* **87,** 163111 (2005).
23. P. Kondratyuk and J.T. Yates: Molecular views of physical adsorption inside and outside of single-wall carbon nanotubes. *Accounts Chem. Res.* **40,** 995 (2007).
24. S.K. Bhatia and D. Nicholson: Anomalous transport in molecularly confined spaces. *J. Chem. Phys.* **127,** 124701 (2007).
25. N.W. Ockwig and T.M. Nenoff: Membranes for hydrogen separation. *Chem. Rev.* **107,** 4078 (2007).
26. J.C.M. Li: Damping of water infiltrated nanoporous glass. *J. Alloys Compd.* **310,** 24 (2000).
27. M.J. Decker, C.J. Halbach, C.H. Nam, N.J. Wagner, and E.D. Wetzel: Stab resistance of shear thickening fluid treated fabrics. *Compos. Sci. Technol.* **67,** 565 (2007).
28. Y.S. Lee, E.D. Wetzel, and N.J. Wagner: The ballistic impact characteristics of Kevlar woven fabrics impregnated with a colloidal shear thickening fluid. *J. Mater. Sci.* **38,** 2825 (2003).
29. F.Q. Yang: Flow behavior of an Eyring fluid in a nanotube—The effect of the slip boundary condition. *Appl. Phys. Lett.* **90,** 133105 (2007).
30. G.G. Wildgoose, C.E. Banks, H.C. Leventis, and R.G. Compton: Chemically modified carbon nanotubes for use in electroanalysis. *Microchem. Acta* **152,** 187 (2006).
31. A. Han, X. Kong, and Y. Qiao: Pressure induced infiltration in nanopores. *J. Appl. Phys.* **100,** 014308 (2006).
32. Y. Qiao, G. Cao, and X. Chen: Effects of gas molecules on nanofluidic behaviors. *J. Am. Chem. Soc.* **129,** 2355 (2007).